Characterization of Cobalt(II)-Substituted Peptide Deformylase: Function of the Metal Ion and the Catalytic Residue Glu-133†

P. T. Ravi Rajagopalan, Stephanie Grimme, and Dehua Pei*

Department of Chemistry, The Ohio State University, 100 West 18th Avenue, Columbus, Ohio 43210

Received August 24, 1999; Revised Manuscript Received November 9, 1999

ABSTRACT: Peptide deformylase (PDF) catalyzes the hydrolytic removal of the N-terminal formyl group from nascent ribosome-synthesized polypeptides in eubacteria. PDF represents a novel class of mononuclear iron protein, which utilizes an Fe^{2+} ion to catalyze the hydrolysis of an amide bond. This Fe^{2+} enzyme is, however, extremely labile, undergoing rapid inactivation upon exposure to molecular oxygen, and is spectroscopically silent. In this work, we have replaced the native Fe^{2+} ion with the spectroscopically active Co^{2+} ion through overexpression in the presence of Co^{2+}. Co^{2+}-substituted PDF (Co-PDF) has an activity 3−10-fold lower than that of the Fe^{2+}-PDF but is highly stable. Steady-state kinetic assays using a series of substrates of varying deformylation rates indicate that Co-PDF has the same substrate specificity as the native enzyme. Co-PDF and Fe-PDF also share the same three-dimensional structure, pH sensitivity, and inhibition pattern by various effector molecules. These results demonstrate that Co-PDF can be used as a stable surrogate of Fe-PDF for biochemical characterization and inhibitor screening. The electronic absorption properties of the Co^{2+} ion were utilized as a probe to monitor changes in the enzyme active site as a result of site-directed mutations, inhibitor binding, and changes in pH. Mutation of Glu-133 to an alanine completely abolishes the catalytic activity, whereas mutation to an aspartate results in only ∼10-fold reduction in activity. Analysis of their absorption spectra under various pH conditions reveals pK_a values of 6.5 and 5.6 for the metal-bound water in E133A and E133D Co-PDF, respectively, suggesting that the metal ion alone is capable of ionizing the water molecule to generate the catalytic nucleophile, a metal-bound hydroxide. On the other hand, substrate binding to the E133A mutant induces little spectral change, indicating that in the E·S complex the formyl carbonyl oxygen is not coordinated with the metal ion. These results demonstrate that the function of the active-site metal is to activate the water molecule, whereas Glu-133 acts primarily as a general acid, donating a proton to the leaving amide ion during the decomposition of the tetrahedral intermediate.

Protein synthesis in prokaryotes initiates with an *N*-formylmethionyl-$tRNA_i$, resulting in N-terminal formylation of all nascent polypeptides (*1*). Peptide deformylase (PDF)[1] catalyzes the subsequent removal of the formyl group from the majority of bacterial proteins (*2*−*4*). Genetic studies have shown that PDF activity is essential for bacterial survival (*5*, *6*). Since PDF is apparently absent in eukaryotic systems, it is currently being pursued as a potential target for designing novel antibacterial drugs.

Biochemical studies of PDF have been plagued in the past by its extreme lability in vitro, which prevented its isolation or characterization for 3 decades (*2*−*4*). Molecular cloning of the deformylase gene (*def* or *fms*) from *Escherichia coli* (*5*) and *Thermus thermophilus* (*6*) and more recently from a variety of other organisms (*7*) permitted its overexpression in *E. coli* and subsequent purification to homogeneity (*8*−*10*). However, the purified enzyme remains unstable ($t_{1/2}$ ∼ 1 min), complicating the kinetic characterization of this enzyme (*8*, *9*). Very recently, biochemical studies have established that PDF represents an new class of metallopeptidase, which utilizes a ferrous ion as the catalytic metal (*9*, *11*). The extraordinary lability of PDF was shown to be due to sensitivity of the catalytic Fe^{2+} ion to environmental oxygen (*12*). To generate a stable PDF variant, several laboratories have replaced the ferrous ion with Zn^{2+} (*8*, *10*, *11*) and Ni^{2+} (*9*, *13*) through in vitro reconstitution or overexpression in defined media. While Zn(II)-PDF has reduced activity by 2−3 orders of magnitude, Ni(II)-substituted PDF retains essentially full catalytic activity of the native enzyme. Both enzyme forms are indeed highly stable, making them invaluable tools for biochemical studies as well as in the screening of potential PDF inhibitors. We have also generated a Co(II)-substituted PDF, in anticipation that the Co(II) ion would provide a useful spectroscopic probe. The Co(II) enzyme has only slightly reduced activity and is very stable. X-ray crystallographic studies of Co(II)-PDF as well as the Zn^{2+}, Ni^{2+}, and Fe^{2+} forms revealed a

† This work was supported by a grant from the National Institutes of Health (AI40575 to D.P.). S.G. was a summer undergraduate researcher supported by the REU program of the National Science Foundation (CHE 9619937).

* Corresponding author: Department of Chemistry, The Ohio State University, 100 W. 18th Ave., Columbus, OH 43210. Telephone: (614) 688-4068. Fax: (614) 292-1532. E-mail: pei.3@osu.edu.

[1] Abbreviations: PDF, peptide deformylase; Co-PDF, cobalt(II)-substituted peptide deformylase; Fe-PDF, Fe^{2+}-containing peptide deformylase; f-ML-*p*NA, *N*-formylmethionylleucyl-*p*-nitroanilide; ML-*p*NA, methionylleucyl-*p*-nitroanilide; thiaPhe, *β*-thiaphenylalanine; LMCT, ligand−metal charge transfer.

10.1021/bi9919899 CCC: $19.00
Published on Web 01/04/2000

virtually identical three-dimensional structure (*7, 14*−*18*). The metal ion is tetrahedrally bound by a water molecule and by the side chains of two histidines of the conserved HExxH motif and of a conserved cysteine.

In this work, we report the detailed biochemical and spectroscopic characterization of Co(II)-substituted PDF of *Escherichia coli*, in comparison to the native Fe(II)-PDF. Our results demonstrate that the cobalt(II)-substituted enzyme can be used as a stable surrogate for studying the structure−function relationship in PDF. Site-directed mutagenesis (*10*) and structural studies (*7, 14*−*18*) have previously identified the residues which are important for catalysis, and a catalytic mechanism has also been proposed. However, the precise function(s) of each individual moiety during catalysis has (have) not been well established. By using the cobalt-substituted enzyme coupled with site-directed mutagenesis, we have elucidated the catalytic functions of the metal cofactor and a conserved glutamate residue (Glu-133) in the enzyme active site.

EXPERIMENTAL PROCEDURES

Buffers. Buffer A, 20 mM MES, pH 6.0, 10 mM NaCl, 1 mM EDTA, 1 mM 1,10-phenanthroline, 10 mM β-mercaptoethanol, 1% Triton X-100 (Sigma), and 0.5% protamine sulfate (Sigma); buffer B, 20 mM MES, pH 6.0, and 10 mM NaCl; buffer C, 20 mM Tris, pH 8.5, and 10 mM NaCl; buffer D, 50 mM potassium phosphate, pH 7.0, and 10 mM NaCl; buffer E, 20 mM Tris, pH 8.0, 0.5 M NaCl, and 5 mM imidazole.

Growth Media. The minimal media contained 2.5 g/L D-(+)-glucose (Sigma), 5 g/L casamino acids (Difco), 10.8 g/L K_2HPO_4, 5.5 g/L KH_2PO_4, 10.0 g/L NaCl, 1.0 g/L ammonium sulfate, 2 mg/L thiamine (Sigma), and 1 mg/L (+)-biotin (Aldrich) and was supplemented with a metal mixture [124 mg/L $MgSO_4 \cdot 7H_2O$, 74 μg/L $CaCl_2 \cdot 2H_2O$, 20 μg/L $MnCl_2 \cdot 4H_2O$, 31 μg/L H_3BO_3, 1.2 μg/L $(NH_4)_6Mo_7O_{24} \cdot 4H_2O$, 1.6 μg/L $CuSO_4$].

Construction of His·Tag PDF and Site-Directed Mutagenesis. Plasmid pET-22b-def (*8*), which contains the entire coding sequence of *E. coli* PDF, was digested with restriction enzymes *Sma*I (which cleaves at 8 bp upstream of the stop codon) and *Xho*I [which cleaves immediately upstream of the $(His)_6$ coding sequence]. The resulting vector DNA was treated with the Klenow fragment of DNA polymerase I, gel-purified, and religated with T4 DNA ligase to give the desired plasmid pET-22b-def-CHT. This construct directs the synthesis of a PDF variant which contains a C-terminal $(His)_6$ tag (designated as PDF-H_6). The two C-terminal residues of wild-type PDF, Arg-167 and Ala-168, were replaced with leucine and glutamate, respectively, as a result of this procedure.

Site-directed mutagenesis was carried out using the QuikChange method (Stratagene). Mutagenesis primers used were the following: E133D, 5′-CCATCTGTATTCAGCATGATATGGATCACCTGGTCGG-3′; E133Q, 5′-CTGTATTCAGCATCAGATGGATCACCTGG-3′; E133C, 5′-GTTAGCCATCTGTATTCAGCATTGTATGGATCACCTGGTCGG-3′. The E133A mutant was constructed by the Kunkel mutagenesis method (*19*) using the primer 5′-GGTGATCCATAGCATGCTGAAT-3′. The mutants were confirmed by sequencing the entire gene.

Purification of Co^{2+}-Substituted PDF. E. coli BL21(DE3) cells carrying plasmid pET-22b-def (*8*) were grown in the minimal media containing 75 mg/L ampicillin at 37 °C until OD_{600} reached ∼0.9 (approximately 3.5 h). The cells were collected by centrifugation (Sorvall GS-3 rotor, 10 min at 5000 rpm) and resuspended in fresh minimal media at 25 °C. After shaking for 10 min, $CoCl_2$ and isopropyl-β-D-thiogalactopyranoside were added to the medium to a final concentration of 100 μM. The resulting culture was shaken at 30 °C for 18 h. The cells (3 L) were harvested by centrifugation and resuspended in 50 mL of buffer A containing 100 μg/mL chicken egg white lysozyme and a protease inhibitor mixture (100 μg/mL phenylmethanesulfonyl fluoride and 20 μg/mL each of trypsin inhibitor, leupeptin, and pepstatin A). From this point on, all of the steps were performed at 4 °C, unless noted otherwise. The cells were lysed by incubation for 30 min, followed by brief sonication (5 × 10 s pulses). The crude lysate was centrifuged (10 min at 15 000 rpm, Sorvall SS-34 rotor) to yield a clear supernatant. The supernatant (∼50 mL) was loaded onto an SP-Sepharose column (Pharmacia Biotech, 2 × 10 cm) which had been equilibrated in buffer B. After washing with buffer B (60 mL), the column was eluted by gravity with 400 mL of buffer B plus a 10−1000 mM NaCl gradient generated via a gradient mixer. Fractions containing significant PDF (located by 12% SDS−PAGE analysis) were pooled and concentrated in a Centriprep-10 apparatus (Amicon). The resulting solution was diluted 10-fold in buffer C and loaded onto a Q-Sepharose column (Pharmacia Biotech, 2 × 10 cm) preequilibrated in buffer C. Elution was carried out with 200 mL of buffer C and a linear gradient of 10−500 mM NaCl at 4 mL/min. PDF active fractions were pooled, concentrated, and dialyzed against 20 mM Tris·HCl buffer (pH 8.0). Typically, the PDF was near homogeneity (as judged by SDS−PAGE analysis) at this stage and was used without further purification. Occasionally, the PDF was further purified on a Phenyl Sepharose column (Pharmacia HR10/16) to remove a small amount of Zn(II)-substituted PDF. The separation between Co^{2+}-PDF and Zn^{2+}-PDF on this column is analogous to the separation between Zn vs Fe(II) PDF (*11*). After the purification was completed, the protein was dialyzed against a metal-free buffer (20 mM Hepes, pH 7.0, 50 mM NaCl) and stored frozen at −80 °C.

Expression of the C-terminal His-tagged wild-type and mutant PDF was carried as described above. After SP-Sepharose and Q-Sepharose purification, the Co^{2+}-PDF-H_6 sample was dialyzed against buffer E and loaded by gravity flow onto a Talon cobalt affinity resin column (Clontech, 2 × 7 cm). The column was washed with 10 column volumes of buffer E, and the bound proteins were eluted with 2 column volumes of buffer E containing 60 mM imidazole. The eluted protein was dialyzed against 20 mM Tris·HCl buffer (pH 8.0) to remove the imidazole and any cobalt bound to the histidine tag. For each sample prepared, metal analysis was performed by inductively coupled plasma emission spectrometry (ICP-ES) at the Chemical Analysis Laboratory of The University of Georgia.

PDF Assays. Co^{2+}-PDF and Fe^{2+}-PDF were assayed under ambient conditions using three different methods depending on the substrate involved. Method A was employed for f-ML-*p*NA and Ac-ML-*p*NA, in which the deformylase reaction was coupled to an aminopeptidase reaction (*20*). Method B

was used for other *N*-formylmethionyl peptides, and the release of the N-terminal amine was monitored with 2,4,6-trinitrobenzenesulfonic acid (*9*). Method C was used for *N*-formyl-*β*-thiaphenylalanyl peptides; deformylation of these peptides results in the release of a thiophenol molecule which was quantitated using Ellman's reagent (*21*).

pH Profile. PDF activity was measured with f-ML-*p*NA (18 μM) (method A). The amount of PDF used in the assays was 2.3 nM for wild-type Co-PDF and 6.6−66 nM for E133D Co-PDF, whereas the amount of *Aeromonas* aminopeptidase used was 0.5−5 units/mL. The reaction was monitored continuously at 405 nm, and the initial rate was calculated from the early portion of the reaction progress curve (30−300 s). The substrate to product conversion during this period was kept at <5%. All buffers contained 20 mM buffer material and 2.0 M NaCl. The buffers used were as follows: pH 4.1−5.5, sodium acetate; pH 5.5−6.5, Mes; pH 6.6−7.5, Mops; pH 7.6−8.5, Tricine; pH 8.6−9.9, Ches; pH 10.0−11.4, sodium bicarbonate. The extinction coefficient of *p*-nitroaniline at 405 nm was constant over the pH range tested ($\epsilon = 1.06 \times 10^4$ M^{-1} cm^{-1}). The experimental data were fitted to eq 1:

$$k_{cat}/K_M = (k_{cat}/K_M)^{lim}/[1 + H/K_{a1} + K_{a2}/H] \quad (1)$$

where $(k_{cat}/K_M)^{lim}$ is the pH-independent second-order rate constant, H is the proton concentration, and K_{a1} and K_{a2} are the ionization constants of the free enzyme. The substrate does not undergo any ionization event that affects the catalytic rate in the pH range tested.

To determine the effect of pH on the K_M value, assay reactions were similarly carried out with f-ML-*p*NA (5.8−180 μM). The same set of buffers as described above was used but contained 50 mM NaCl (500 mM NaCl for wild-type PDF at pH 5.5). The amount of PDF used in the assay reaction was 2.0 nM for wild-type Co-PDF and 9.4−94 nM for E133D Co-PDF. The k_{cat} and K_M values under various pH conditions were obtained by fitting the observed initial rates against the Michaelis−Menten equation. The k_{cat} values exhibited the same pH dependence as the k_{cat}/K_M value from above.

Absorption Spectroscopy. All absorption spectra were recorded on a Perkin-Elmer Lambda 20 UV−vis spectrophotometer at room temperature. PDF samples were prepared in buffers of various pH as described above to give a final concentration of 50−250 μM and transferred into a 100 μL quartz microcuvette. Buffers containing high salt concentrations were prepared separately from the corresponding low-salt solutions, and their pH values were carefully measured by pH meters. When PDF substrates or inhibitors were added to the PDF samples, the pH values were again examined by either pH meter or pH paper to ensure that there was no pH drift.

Determination of Binding Constants. Wild-type or E133 mutant Co-PDF (50−135 μM) was dissolved in 100 mM Tris·HCl buffer (pH 8.0) containing 0−3.5 mM thiorphan or 2-mercaptoethanol, and their absorbance values at 328 or 670 nm were determined. The dissociation constants (K_D) were determined by fitting experimental data (absorbance increase, ΔA) against the equation: $\Delta A = \Delta A_{max}[I]/(K_D + [I])$, where ΔA_{max} is the maximum increase in absorbance at saturating concentration of the inhibitor. A K_D of 148 ± 35 μM was obtained for binding of 2-mercaptoethanol to E133A PDF. To determine the binding affinity of f-ML-*p*NA to E133A PDF, the protein ($E_0 = 135$ μM) was first mixed with saturating amounts of 2-mercaptoethanol ($I_0 = 1.2$ mM), and the maximum absorbance increase at 670 nm (ΔA_{max}) was measured. Next, increasing concentrations of f-ML-*p*NA ($S_0 = 40-160$ μM) were added to the above solution, and the absorbance increase (ΔA) at 670 nm was determined for each f-ML-*p*NA concentration. The K_D value for f-ML-*p*NA was determined by eq 2:

$$K_D = K_D'\Delta A\{S_0 - E_0[(\Delta A_{max} - \Delta A)/\Delta A_{max}]/[(\Delta A_{max} - \Delta A)I_0]\} \quad (2)$$

where K_D' is the dissociation constant of 2-mercaptoethanol (148 μM).

To determine the binding affinity of chloride ion to the active-site metal, wild-type or E133 mutant Co-PDF was dialyzed exhaustively against chloride-free buffers prior to use. The resulting protein sample (50−200 μM) was adjusted to contain 0−3.3 M NaCl. The pH value of the resulting solution was checked on a pH meter and adjusted when necessary to ensure that there was no pH drift. The absorption spectra of the samples (120 μL) were recorded, and the absorbance at 605 nm, A, was plotted against the chloride concentration, [Cl]. The apparent dissociation constant, K_D, was determined by fitting the experimental data against eq 3:

$$A = A_0 + A_{max}[Cl]/(K_D + [Cl]) \quad (3)$$

where A_0 is the absorbance at 605 nm in the absence of NaCl and A_{max} is the maximum absorbance at 605 nm in the presence of saturating concentrations of NaCl. The buffers used were 100 mM Mes for pH 6.0, 100 mM Mops for pH 6.7, and 100 mM Tris−acetate for pH 8.0.

RESULTS

Preparation of Co(II)-Substituted PDF. We initially attempted to substitute Co^{2+} for Zn^{2+} by direct exchange dialysis, but it was not successful because the Zn^{2+} metal was tightly bound and can only be removed by guanidine hydrochloride denaturation. Refolding of the denatured Zn-PDF in the presence of Co^{2+} did afford active Co(II)-substituted PDF, but the highest Co^{2+}:Zn^{2+} ratio obtained was ~1:1. This is due to the difficulty in completely denaturing Zn-PDF. Meanwhile, Groche et al. (*9*) successfully prepared large amounts of pure Fe-PDF by growing the overproducing cells in minimal medium supplemented with Fe^{2+}. By using a similar growth medium enriched in Co^{2+} (100 μM), we were able to produce predominantly Co-PDF in large quantities (typical yield of 25 mg/L). The Co-PDF was purified in a fashion similar to that of Fe-PDF (see Experimental Procedures). Metal analysis of the purified samples shows that the Co^{2+} content is typically 95% or higher, with the minor metal component being Zn^{2+} (Table 1). The presence of small amounts of Zn^{2+} does not pose a problem to our studies because the Zn-PDF is nearly 2 orders of magnitude less active than the Co-PDF (Table 1) and zinc is spectroscopically silent.

Purification of PDF Mutants by Metal Affinity Chromatography. PDF mutants overexpressed in *E. coli* cells are

Table 1: Metal Contents and Catalytic Activities of PDF Variants[a]

protein	metal/polypeptide Fe	Co	Zn	Cu, Mn, etc.	k_{cat}/K_M (M^{-1} s^{-1})
Fe-PDF (WT)	1.03	0.00	0.07	0.07	$(3.50 \pm 0.20) \times 10^6$
Co-PDF (WT)	0.00	0.95	0.05	0.00	$(1.11 \pm 0.18) \times 10^6$
Zn-PDF (WT)	0.00	0.00	0.96	0.01	$(3.1 \pm 0.7) \times 10^4$
Co-PDF-H_6 (WT)	0.00	0.84	0.10	0.00	$(1.19 \pm 0.07) \times 10^6$
Co-PDF-H_6 (E133D)	0.00	0.85	0.05	0.01	$(1.5 \pm 0.1) \times 10^5$
Co-PDF (E133A)	0.00	0.80	0.03	0.01	2230 ± 153
Co-PDF-H_6 (E133A)	0.00	0.82	0.04	0.01	0.31 ± 0.13

[a] Assay reactions were performed in 50 mM potassium phosphate (pH 7.0) containing 10 mM NaCl.

often contaminated by the wild-type enzyme synthesized from the chromosomal *def* gene. To remove the wild-type PDF contaminant, a six-histidine tag is placed at the N- and C-termini of the plasmid-coded PDF, respectively. Addition of an N-terminal histidine tag drastically reduced the catalytic activity of PDF. The C-terminally histidine-tagged PDF (PDF-H_6) is, however, well expressed and has identical physical and catalytic properties as the wild-type enzyme. For example, Co-PDF has a k_{cat} value of 19 s^{-1}, K_M of 18 μM, and k_{cat}/K_M of 1.1×10^6 M^{-1} s^{-1} toward f-ML-*p*NA. The corresponding k_{cat}/K_M value for Co-PDF-H_6 toward f-ML-*p*NA 1.2×10^6 M^{-1} s^{-1} (Table 1). Meinnel et al. have previously shown that the C-terminal 22 residues can be removed with no effect on PDF activity (*22*). The addition of the C-terminal histidine tag permits its separation from wild-type PDF on a cobalt affinity column (*23*). This is illustrated by the large difference in activity between Co-PDF(E133A) and Co-PDF-H_6 (E133A) (Table 1), where the former was contaminated with the wild-type activity. Unless noted otherwise, all of the kinetic experiments in this work used mutants that contained the C-terminal histidine tag, whereas proteins without any histidine tag were used for spectroscopic characterization (with the exception of E133D Co-PDF-H_6).

Comparison of Fe-PDF and Co-PDF Properties. We have previously shown that native PDF is likely an Fe^{2+}-containing enzyme, which is highly unstable ($t_{1/2} \sim 1$ min at room temperature) due to oxidation of the catalytic Fe^{2+} ion into the catalytically inactive Fe^{3+} ion by molecular oxygen (*12*). Therefore, a motivating reason behind this work is to find a PDF variant that is stable enough to permit detailed mechanistic investigations. To our delight, Co(II)-substituted PDF is highly stable; it can be stored for hours to days at 4 °C or at room temperature exposed to environmental oxygen without any loss of activity. It is worth mentioning that the Zn(II)- and Ni(II)-substituted PDF enzymes are also highly stable (*8*−*13*). Thus, the extraordinary lability of PDF appears to be uniquely associated with the Fe-PDF form, providing further support that Fe-PDF is most likely the physiological form. Co-PDF is denatured at ~2.2 M guanidine hydrochloride ($MC_{50} = 2.2$ M), placing its stability between those of Fe-PDF ($MC_{50} = 1.7$ M) and Zn-PDF ($MC_{50} = 2.6$ M). The circular dichroism spectrum of Co-PDF is identical to that of Fe-PDF (not shown). Finally, the X-ray crystal structure of Co-PDF has been determined to 2.1 Å resolution and shows no structural difference from the Zn-PDF, Ni-PDF, or Fe-PDF forms (*18*).

The catalytic properties of Co-PDF were evaluated with a diverse set of substrates which have catalytic efficiencies differing by 6 orders of magnitude (Table 2). Co-PDF is highly active. For example, the k_{cat}/K_M for f-ML-*p*NA is 1.1×10^6 M^{-1} s^{-1}, only 3-fold lower than that of Fe-PDF. The cobalt enzyme shows the same substrate specificity as Fe-PDF, with its catalytic activities toward all of the tested substrates consistently 3−10-fold lower than those of the iron enzyme (Table 2). Both Co-PDF and Fe-PDF show similar pH dependence in their catalytic activities (see below). Co-PDF was also inhibited by 1,10-phenanthroline and a transition-state analogue inhibitor, (*S*)-2-*O*-(H-phosphonoxy)-L-caproyl-L-leucyl-*p*-nitroanilide (*24*), with similar inhibition constants (<5-fold difference) to those of Fe-PDF (data not shown). Taken together, the above results suggest that substitution with Co^{2+} has not significantly altered the catalytic properties of PDF. Therefore, Co-PDF provides a reasonable surrogate for mechanistic investigations.

Catalytic Properties of E133 Mutants. Glu-133 is the second residue of the "signature" motif, HExxH, which is universally conserved among all PDFs from over 2 dozen distantly related bacterial organisms (*7*). To assess its role during catalysis, Glu-133 was mutated to alanine, aspartate, cysteine, and glutamine. The E133A and E133D mutants were well expressed and gave soluble proteins that were purified to homogeneity, whereas the E133C and E133Q mutants failed to produce soluble protein. Surprisingly, mutation of Glu-133 to aspartate resulted in only a modest reduction in activity, less than 10-fold for most of the substrates tested (Table 2). The decrease in activity is primarily due to a decrease in the k_{cat} value, whereas the K_M value is essentially unchanged. In contrast to the high activity of the E133D mutant, mutation of Glu-133 to alanine resulted in 10^7-fold reduction in activity, having a k_{cat}/K_M value of 0.31 M^{-1} s^{-1} toward f-ML-*p*NA (Table 1). We believe that E133A PDF is catalytically inactive and the residual activity observed is likely due to a small amount of active contaminant that was not removed by metal chelation chromatography or was produced by translational misincorporation during ribosomal protein synthesis (*25*).

pH Profile Analysis. The pH dependence of wild-type and E133D PDF was studied using f-MA, f-ML-*p*NA, f-β-thiaPhe-Lys-pNA (*21*), and f-β-thiaPhe-OBn (*21*) as substrates, which all gave essentially identical pH profiles. These studies were somewhat complicated by the fact that PDF undergoes denaturation under acidic conditions, as evidenced by loss of activity as well as protein precipitation at pH <5.5. Increase in the ionic strength of the buffer was found to stabilize the protein, and therefore the pH profile studies were carried out in the presence of 2 M NaCl. Figure 1 shows the pH profiles of wild-type Co-PDF, and E133D Co-PDF-H_6 determined with f-ML-*p*NA as substrate. The K_M values of the two enzymes are similar to each other (~2-fold higher for E133D PDF), and both are pH-independent (Figure 1A). Therefore, the pH profile of the reaction velocity (V) at 18 μM substrate represents the pH dependence of the k_{cat} value (Figure 1B). Wild-type Co-PDF exhibits a flat pH profile from pH 6.5 to 11.6. At pH <6.5, PDF activity decreases with pH. Data fitting indicates the titration of a single active-site group with an apparent pK_a of 5.7. When the experiments were carried out in the presence of 50 mM NaCl (instead of

Table 2: Catalytic Activity of Various PDFs toward Peptide Substrates[a]

enzyme	substrate[b]	k_{cat} (s^{-1})	K_M (μM)	$k_{cat}/K_M \times 10^{-3}$ (M^{-1} s^{-1})	relative k_{cat}/K_M[c]
Fe-PDF (WT)	f-Met-Leu-*p*NA	70 ± 2	20.3 ± 1.3	3500 ± 200	
	f-Met-Ala	−	−	8.82 ± 0.86	
	Ac-Met-Leu-*p*NA	−	−	0.025 ± 0.001	
	f-Met	−	−	0.0051 ± 0.0006	
	f-Met-Leu-NH_2	1320 ± 40	2640 ± 190	500 ± 90	
	f-thiaPhe-OBn	−	−	6.20 ± 0.30	
	f-thiaPhe-Leu-*p*NA	−	−	690 ± 30	
	f-thiaPhe-Lys-*p*NA	86 ± 6	27.1 ± 5.9	3200 ± 500	
Co-PDF (WT)	f-Met-Leu-*p*NA	19.1 ± 1.9	17.8 ± 3.3	1110 ± 180	0.32
	f-Met-Ala	−	−	0.80 ± 0.10	0.09
	Ac-Met-Leu-*p*NA	−	−	0.0086 ± 0.0004	0.35
	f-Met	−	−	0.00029 ± 0.00013	0.06
	f-Met-Leu-NH_2	1280 ± 90	7360 ± 800	170 ± 60	0.35
	f-thiaPhe-OBn	−	−	1.04 ± 0.08	0.17
	f-thiaPhe-Leu-*p*NA	−	−	62 ± 1	0.09
	f-thiaPhe-Lys-*p*NA	13.3 ± 0.4	29.9 ± 0.8	445 ± 2	0.14
Co-PDF (E133D)	f-Met-Leu-*p*NA	4.2 ± 0.1	28.1 ± 0.6	150 ± 10	0.14
	f-Met-Ala	−	−	0.0075 ± 0.0015	0.01
	f-thiaPhe-OBn	−	−	0.49 ± 0.01	0.50
	f-thiaPhe-Leu-*p*NA	−	−	7.90 ± 0.20	0.13
	f-thiaPhe-Lys-*p*NA	0.99 ± 0.01	18.2 ± 0.7	55 ± 1	0.12

[a] All assay reactions were carried out in 50 mM potassium phosphate (pH 7.0) containing 10 mM NaCl. Data presented are the mean ± SD from three independent sets of experiments. [b] f-Met-Leu-*p*NA, *N*-formylmethionylleucyl-*p*-nitroanilide; Ac-Met-Leu-*p*NA, *N*-acetylmethionylleucyl-*p*-nitroanilide; f-thiaPhe-OBn, *N*-formyl-β-thiaphenylalanyl benzyl ester; −, no saturation under conditions used in this work. [c] For wild-type Co-PDF, the activities are relative to those of wild-type Fe-PDF, whereas for E133D Co-PDF the activities are relative to those of wild-type Co-PDF.

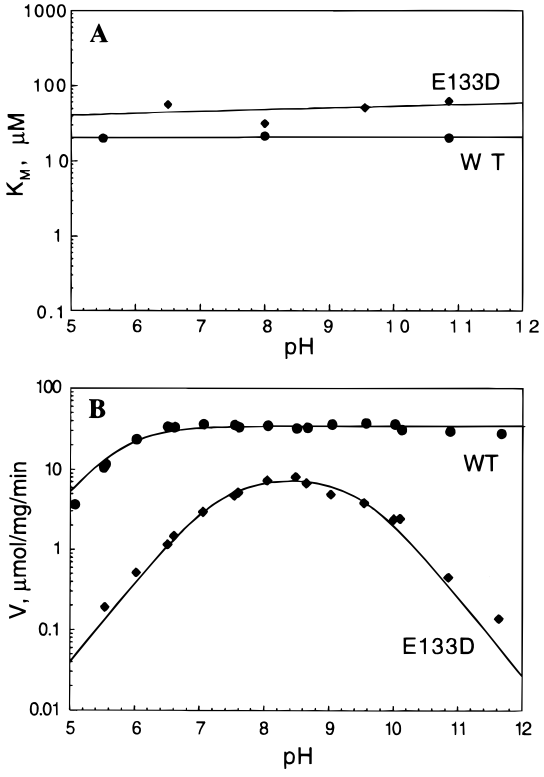

FIGURE 1: Effect of pH on (A) the K_M value and (B) the k_{cat}/K_M value for wild-type (circles) and E133D PDF (squares). The lines drawn (in panel B) through the experimental data were based on the nonlinear least-squares fit to the equations described under Experimental Procedures.

2 M NaCl), the pH profile was qualitatively similar, but the apparent pK_a decreased to ~5.2 (this value was, however, complicated by partial denaturation of the enzyme at pH <5.5). Wild-type Fe-PDF has the same pH profile as Co-PDF. For the E133D mutant, the activity increases with pH before reaching a plateau at pH 7.5 (Figure 1B). This again reflects the titration of a single group with an apparent pK_a of 7.3, which was shifted to ~6.0 in the presence 50 mM NaCl. Unlike the wild-type enzyme, the mutant exhibits a decreasing trend at pH >9 (pK_a = 9.5). This is likely due to the deprotonation of D133 at basic pH, rendering the enzyme inactive. The pH profile of E133A PDF could not be determined due to lack of activity.

Absorption Spectroscopy. Substitution of Co^{2+} for the native metal in a metalloenzyme provides a useful spectroscopic probe of the enzyme active-site environment. This technique has previously been employed to successfully characterize numerous metalloenzymes (*26*). Figure 2 shows the electronic absorption spectra of Co(II)-substituted wild-type, E133D, and E133A PDF under various pH conditions. The spectrum of wild-type PDF shows an intense absorption at 325 nm (ϵ = 1100 M^{-1} cm^{-1}), likely due to the ligand-to-metal charge transfer (LMCT) from the ligating cysteine-90 to the Co^{2+}. The magnitude of the extinction coefficient is consistent with a spin- and symmetry-allowed transition by the selection rules. In the visible region, PDF exhibits three bands at 565, 640, and 660 nm which can be attributed to Co(II) d−d transitions. Empirical observations for Co(II) complexes with well-defined coordination spheres suggest that the extinction coefficient of the d−d transition absorptions can be used as an indicator of the coordination number (*27*): ϵ > 300 M^{-1} cm^{-1} for a four-coordinate complex; 50 < ϵ < 300 M^{-1} cm^{-1} for a five-coordinate site; and $\epsilon \leq$ 50 M^{-1} cm^{-1} for a six-coordinate site. The extinction coefficient of 580 M^{-1} cm^{-1} (at 565 nm) for Co-PDF suggests that the Co^{2+} ion in PDF is four-coordinate. This agrees with the crystal structure of Co-PDF, in which the metal ion is tetrahedrally coordinated by His-132, His-136, and Cys-90 from the protein and a water molecule (*14*−*18*). A weak transition was also observed in the near-infrared region (ϵ

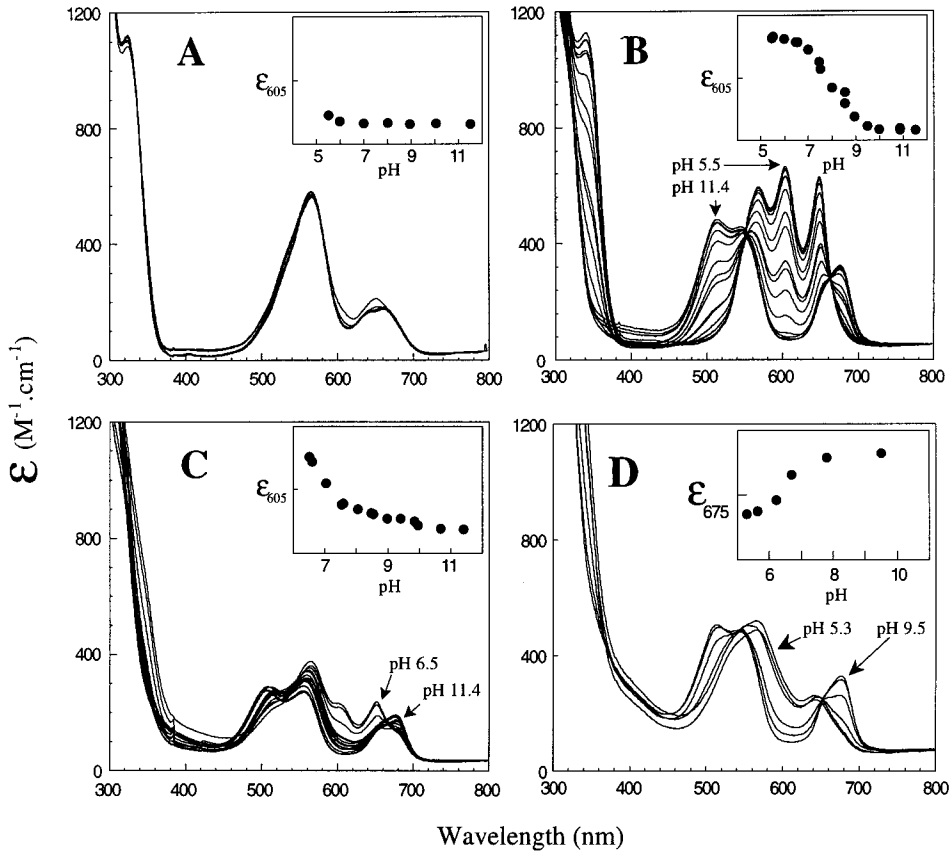

FIGURE 2: UV-visible spectra of Co-PDF under various pH and salt conditions. (A) Wild-type PDF at pH 5.5−11.4, 50 mM NaCl; (B) E133A PDF at pH 5.5−11.4, 50 mM NaCl; (C) E133D PDF at pH 6.5−11.4, 50 mM NaCl; and (D) E133A PDF in chloride-free buffers (pH 5.3−9.5). Insets: plot of absorbance at 605 nm (675 nm in panel D) against pH.

$\sim$ 45 M^{-1} cm^{-1} at 930 nm), corresponding to the $^4A_2$ to $^4T_1(F)$ transition. Strikingly, the wild-type spectra show no significant changes when the pH of the solution was titrated from 5.5 to 11.4 (Figure 2A), suggesting the absence of any ionization event near the active site. This is, however, consistent with the pH insensitivity of PDF activity in this range.

The absorption spectra of the E133D and E133A mutants (in the presence of 50 mM NaCl) are similar to each other but significantly different from that of wild-type Co-PDF and are pH-sensitive (Figure 2B,C). At basic pH (pH >10), both spectra show absorption bands at 510, 550, and 675 nm, and a shoulder at 650 nm. These spectra are very similar to that of Co(II)-substituted carbonic anhydrase at high pH, where the Co^{2+} ion is tetrahedrally coordinated by three histidyl residues and a hydroxide ion (*28*). At acidic pH (pH $\leq$6), the spectra are entirely different, showing three strong, sharp bands at 565, 605, and 650 nm (ϵ > 600 M^{-1} cm^{-1}). At intermediate pH, the spectra clearly represent the composite spectra of two independent species in varying proportions. The presence of two isobestic points at 555 and 665 nm is indicative of the direct interconversion between two species (no intermediates) as a function of pH. When the absorbance change at 605 nm was plotted against pH, a simple sigmoidal curve was obtained for each mutant, corresponding to the change of a single functional group in the active site (Figure 2B,C insets). Form the titration curve midpoints, apparent pK_a values of 8.0 and $\sim$6.0 were obtained for the E133A and E133D mutants, respectively. The latter pK_a value ($\sim$6.0) agrees quite well with the pK_a value derived from the activity−pH profile ($\sim$6.0). This transition has been assigned to the exchange of the metal-bound hydroxide into metal-bound chloride ion (see Discussion). For both mutants, increase in pH also caused a blue shift in the LMCT band, from 340 nm at pH $\leq$6.5 to 310 nm at pH $\geq$9.0, but no change in the band intensity (Figure 2B,C). The presence of the LMCT band over the entire pH range suggests that pH changes did not disrupt the interaction between the metal ion and the thiolate group of Cys-90.

To determine the actual pK_a value for the metal-bound water, E133A Co-PDF was dialyzed exhaustively against a chloride-free buffer, and its absorption spectra were then recorded at various pHs (Figure 2D). At pH 9.5, the chloride-free spectrum is identical to that obtained in the presence of 50 mM NaCl (same pH). However, at acidic pH (e.g., pH 5.3), a new spectrum emerged, with an absorption maximum at 570 nm and a shoulder at 645 nm. This spectrum is clearly different from that of the metal-bound chloride form or of the metal-hydroxide form (Figure 2B) and is assigned as the enzyme with a metal-bound water molecule (see Discussion). The existence of two isosbestic points at 653 and $\sim$540 nm again indicates that the observed spectral changes with pH are caused by the interconversion between the metal-bound water and metal-bound hydroxide forms. Plot of the absorbance at 675 nm against pH produces a titration curve with a pK_a of 6.5 (Figure 2D inset). This suggests that the active-site metal ion is capable of generating a metal-bound hydroxide under physiological conditions. Remarkably, the E133A spectrum at pH 5.3 closely resembles the spectrum of wild-type Co-PDF, suggesting that in the wild-type active

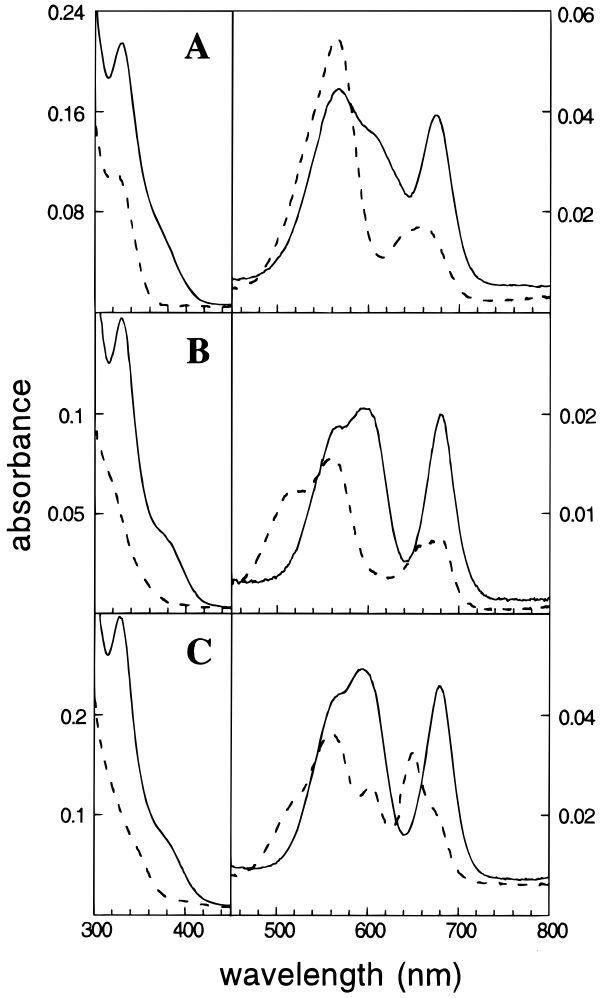

FIGURE 3: UV−visible spectra of wild-type (panel A), E133A (panel B), and E133D Co-PDF (panel C) in the absence (dashed lines) and presence (solid lines) of 4.2 mM thiorphan. The protein samples (52−128 μM) were prepared in 100 mM Tris·HCl (pH 8.0).

site a water molecule is bound to the metal ion under pH 5.5−11.4. Similar pH titration experiments were performed with E133D Co-PDF in chloride-free buffers, and an upper pK_a limit of 6.5 (pK_a < 6.5) was obtained for the metal-bound water (this mutant denatures at pH <6.5).

Spectral Perturbations of Co-PDF by Effector Molecules/Ions. The availability of the spectroscopic probe in Co-PDF permitted us to examine its interaction with substrates, inhibitors, and other molecules/ions that may interact with the enzyme active site. Thiorphan is a weak, thiol-containing inhibitor of PDF (K_I = 189 μM to Ni-PDF) (*29*). We thus employed thiorphan to probe whether the E133D or E133A mutation has caused significant structural perturbation to the PDF active site. Figure 3 shows the spectral changes for both wild-type and mutant PDF upon the addition of excess thiorphan. Although the overall spectra of the thiorphan complexes are somewhat different between wild-type and mutant enzymes, they all show similar changes with respect to the free enzymes. First, the absorbance at 325 nm increases dramatically in intensity (it approximately doubled in the case of wild-type PDF), signifying the ligation of the thiorphan thiol to the Co^{2+} ion. Second, the d−d bands exhibit both a red shift in absorbance wavelength and an increase in intensity, a characteristic feature for sulfur binding

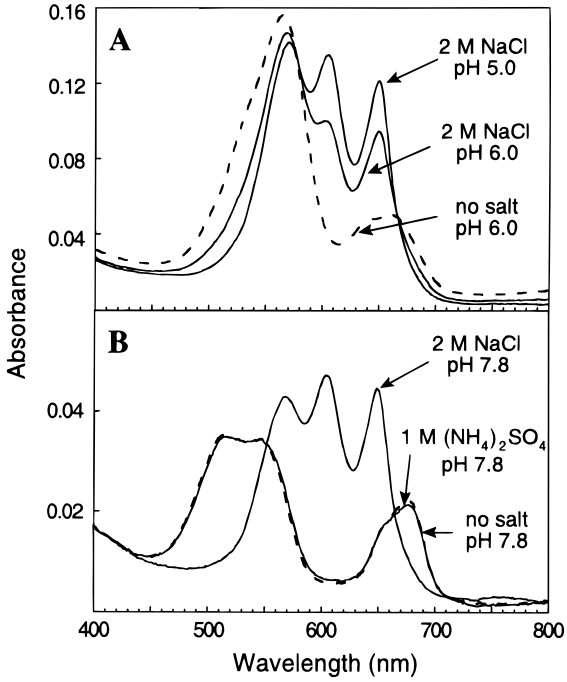

FIGURE 4: Effect of NaCl salt on the UV−visible spectra of wild-type (panel A) and E133A Co-PDF (panel B). The dashed lines represent the spectra in chloride-free buffers (100 mM Mes for pH 6.0 and 100 mM Tricine for pH 7.8).

to cobalt sites (*26*). Finally, a new band at 380 nm appears in all three spectra. Note that the spectra of thiorphan complexes of E133D and E133A mutants are essentially identical.

We next determined the binding affinity of thiorphan to wild-type and mutant PDF by titrating the enzyme with increasing concentrations of the inhibitor and monitoring the absorbance at 328 nm. Dissociation constants (K_D) of 470 ± 60 μM, 63 ± 10 μM, and 73 ± 27 μM were found for wild-type, E133D, and E133A PDF, respectively. Based on the fact that the two E133 mutants have similar absorption spectra in both the free form and the thiorphan-bound form and have similar binding constants to thiorphan, and that E133D PDF has significant catalytic activity, we conclude that the E133D and E133A mutations do not result in significant structural perturbation in the active site.

Monovalent anions (e.g., Cl^-, Br^-, and CN^-) have been shown to perturb the spectra of Co(II) complexes such as carbonic anhydrase (*28*). Addition of 2 M NaCl had little effect on the spectrum of wild-type Co-PDF at pH ≥7 (data not shown). At pH <7, the addition of 2 M NaCl resulted in the replacement of the metal-bound water by a chloride ion, as evidenced by the dramatic spectral changes (Figure 4A). As the chloride-bound enzyme is likely catalytically inactive, we believe that inhibition by chloride ion at acidic pH is partially responsible for the decreasing trend toward acidic pH observed in the activity−pH profile (Figure 1). The E133D and E133A mutants underwent dramatic spectral changes upon the addition of 2 M NaCl, and the changes occurred at any pH in the range of pH 5.0−11.4. Figure 4B shows the spectral changes for the E133A mutant; similar changes were observed for the E133D mutant. At pH 7.8 and in the absence of chloride ions, the E133A enzyme exists primarily in the metal-hydroxide form. In the presence of 2 M NaCl (pH 7.8), the 510 and 675 nm bands, which are the

distinctive features of the Co(II)-hydroxide species, completely disappeared. Three new bands appeared at 565, 605, and 650 nm, with a concomitant increase in absorption intensity. This spectrum (at pH 7.8 and in the presence of 2 M NaCl) is identical to that of E133A PDF at acidic pH and in the presence of 50 mM NaCl (Figure 2B). The same type of spectral perturbation by chloride ions was also observed at pH 6.0, pH 9.6, and pH 11.4 (although at pH 9.6 and 11.4 the protein was only partially converted into the metal-bound chloride form by the addition of 2 M NaCl). In a control experiment (at pH 7.8), the addition of 1 M ammonium sulfate had no effect on the E133A PDF spectrum, demonstrating that the observed spectral changes were not due to a simple change in the ionic strength. The simplest explanation is that the hydroxide (water molecule) and chloride ions compete for binding to the same coordination site on the metal ion and the addition of 2 M NaCl shifted the equilibrium toward the metal-bound chloride form. The sulfate anion is presumably too bulky to be accommodated by the PDF active site.

The binding affinity of Cl^- ion to wild-type and mutant Co-PDF was determined by monitoring the absorbance increase at 605 nm upon the addition of varying concentrations of NaCl to a chloride-free PDF sample. At pH 8.0, the apparent dissociation constants (K_D) were 3.6 ± 0.7 M and 110 ± 23 mM for E133D and E133A PDF, respectively; no binding to wild-type PDF was detected. Under weakly acidic conditions, chloride ions bind much more effectively, with apparent K_D values of 88 ± 14 (pH 6.7) and 2.5 ± 0.4 mM (pH 6.0) for E133D and E133A Co-PDF, respectively. The affinity of chloride ions for wild-type PDF could not be reliably determined due to protein denaturation at acidic pH. Two conclusions can be drawn from these observations. First, the drastic changes in the apparent K_D values as a function of pH are another manifestation that the hydroxide (water at acidic pH) and chloride ions compete for binding to the same site of the enzyme. Thus, as pH decreases from 8.0 to 6.0 (the hydroxide ion concentration decreases by 100-fold), the apparent K_D value for E133A PDF decreases by ~50-fold. Second, the chloride ion binds to the three enzymes with the following decreasing order of affinity: E133A > E133D ≫ wild-type. Presumably, the carboxylate group of E133 (D133) stabilizes the metal-bound hydroxide ion (water) through either direct hydrogen bonding (e.g., in wild-type PDF) and/or hydrogen bonding via a water bridge (e.g., in E133D PDF). Such interaction(s) would be missing in the E133A mutant or when a chloride ion is bound to the metal. Based on the apparent K_D of 110 mM for chloride binding to E133A PDF at pH 8.0, we estimate that the hydroxide ion binds the active-site metal 1.1×10^5-fold more tightly than the chloride ion [$K_{D(Cl)}/K_{D(OH)} = 1.1 \times 10^5$]. Similarly, the relative affinity of the metal for ^-OH vs H_2O [$K_{D(H2O)}/K_{D(OH)}$] is estimated to be 1.8×10^9, based on the observed pK_a value of 6.5 for the metal-bound water in E133A PDF (in the absence of Cl^-). By using a thermodynamic cycle (Scheme 1), we estimate that Cl^- binds to E133A Co-PDF with 1.7×10^4-fold higher affinity than a water molecule. These results predict that the addition of 50 mM NaCl to E133A PDF would increase the pK_a value for the metal-bound water by 1.2 pH units to 7.7, in agreement with the experimental data (apparent pK_a ~ 8.0 at 50 mM NaCl) (Figure 2B). Similar calculations for the E133D mutant

Scheme 1

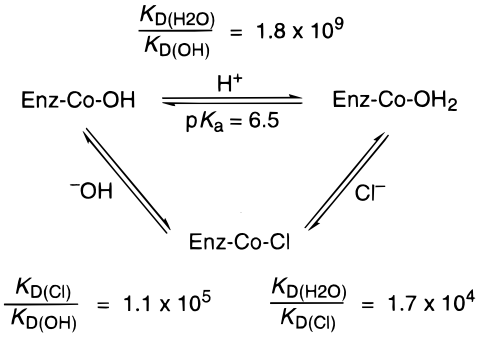

revealed that the hydroxide ion binds to the metal in this enzyme with 4.0×10^6-fold higher affinity than the chloride ion [$K_{D(Cl)}/K_{D(OH)} = 4.0 \times 10^6$]. This predicts that the addition of 50 mM and 2 M NaCl to E133D Co-PDF at pH 6 would increase the apparent pK_a value by 0.35 and 1.7 pH units, respectively. As described above, the apparent pK_a values for the metal-bound water in E133D PDF at 50 mM and 2 M NaCl are ~6.0 and 7.3, respectively (Figures 1 and 2). Subtraction of the pK_a shift due to Cl^- inhibition therefore gives an intrinsic pK_a of 5.6 in both cases. This is again in agreement with the experimental pK_a value (<6.5) obtained from pH titration in the absence of NaCl.

The effect of substrate binding on the spectral property of the E133A mutant was assessed using a high-affinity substrate, f-ML-*p*NA, which has a k_{cat} of 19 s^{-1}, a K_M of 18 μM, and a k_{cat}/K_M value of 1.1×10^6 M^{-1} s^{-1} toward wild-type Co-PDF (Table 2). The K_D for the interaction between f-ML-*p*NA and E133A Co-PDF was determined to be 5.8 ± 0.6 μM, using a competition assay involving 2-mercaptoethanol as a reporter. At pH 6.5, where the protein exists primarily as the metal-bound chloride form, no spectral difference was observed in the presence or absence of 250 μM f-ML-*p*NA (Figure 5A). At pH 9.8, where the predominant species is the metal-bound hydroxide form, the addition of 250 μM f-ML-*p*NA again resulted in essentially no perturbation of the spectrum. There was no change either in the absorbance wavelengths or in the shape of the spectrum. There are only minor changes in absorption intensity, which is partially due to oversubtraction of the background signal (there is a trace amount of *p*-nitroaniline in the substrate). At pH 8.0, where the free enzyme exists as a mixture of the metal-hydroxide and metal-Cl^- forms, spectral changes were observed upon the addition of 250 μM f-ML-*p*NA (Figure 5B). The spectrum of the E·S complex is essentially identical to that of free enzyme at high pH (e.g., pH 9.8). This can best be explained by a substrate-induced conversion of the metal-Cl^- form into the metal-hydroxide form. It also reinforces the notion that the E133A mutant is capable of binding the substrate under these conditions. These results suggest that upon substrate binding there is no change in the inner shell ligands for the metal ion. The high catalytic activity of wild-type and E133D mutant PDF toward f-ML-*p*NA (Table 2) prevented a similar optical titration experiment for these enzyme forms.

DISCUSSION

PDF was recognized as an important enzymatic activity more than 3 decades ago but until recently had totally eluded

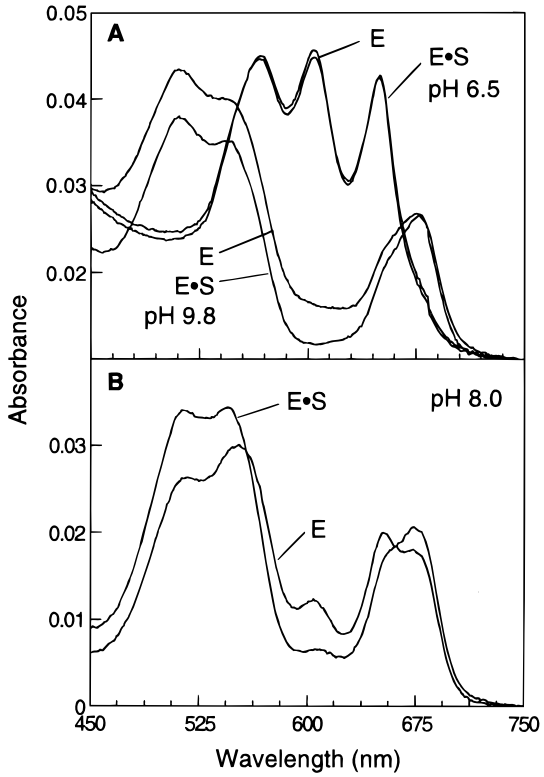

FIGURE 5: Effect of substrate binding (250 μM f-ML-*p*NA) on the UV−visible spectra of E133A Co-PDF (66 μM) at pH 6.5 and 9.8 (panel A) and pH 8.0 (panel B).

purification or characterization. This is due to its extreme sensitivity to molecular oxygen, which instantaneously oxidizes the Fe^{2+} cofactor into catalytically inactive Fe^{3+} ion (*12*). The lability of PDF complicates both kinetic assays and its spectroscopic characterization, as it forms a precipitate upon inactivation (*12*). Also, native PDF is essentially silent spectroscopically. Apart from a weak LMCT band at ~295 nm ($\epsilon \sim 500\ M^{-1}\ cm^{-1}$), Fe-PDF has no detectable absorption in the visible region and is EPR-silent (*11*). In this work, we have replaced the Fe^{2+} ion with Co^{2+} ion, and the resulting Co(II)-substituted PDF retains essentially wild-type activity and substrate specificity. In fact, Co-PDF has a three-dimensional structure that is indistinguishable from that of Fe-PDF (*17, 18*) and shares many of the important properties of the native enzyme including an identical pH profile and sensitivity to PDF inhibitors. A major difference is that the Co-PDF is highly stable, providing a useful surrogate for mechanistic investigation and PDF inhibitor screening. In addition, the electronic properties of the Co(II) ion are highly dependent upon the identity and the symmetry of its ligand environment, providing a sensitive spectroscopic probe for studying the structure−function relationship in this enzyme. Indeed, numerous metalloenzymes (Zn^{2+} enzymes in particular) have been reconstituted with Co(II) ion (*26*). The cobalt-substituted enzymes are almost always active (in some cases hyperactive) and have provided significant mechanistic insights into these enzymes. Because of the extensive structural and functional similarities between Co-PDF and Fe-PDF, we believe that the mechanistic insights gained through the cobalt enzyme should be relevant to the native PDF.

Spectral and pK_a Assignments. The insensitivity of wild-type PDF to pH changes forced us to examine the E133A and E133D mutants, whose catalytic and spectral properties are pH-dependent. In the absence of inhibitory anions (e.g., Cl^-), pH titration of the E133A PDF spectrum at 605 nm produces a sigmoidal curve with a pK_a of 6.5, indicative of a single ionization event near the metal center. The 3D structure of PDF shows a largely hydrophobic active site; the only ionizable groups are the metal-bound water and the side chains of Cys-90, Glu-133, His-132, and His-136 (*7, 14*−*18*). Because wild-type PDF does not show such a pH dependence at pH >5.5, Cys-90, His-132, or His-136 is unlikely to be the ionizing group. Glu-133 cannot be the ionizing group either, as it is absent in E133A PDF. Thus, the only likely candidate for the ionizing group is the metal-bound water. In principle, the observed spectral changes could also be caused by pH-dependent changes in the protein ligands or the geometry of the metal complex (*26, 27*). The 3D structure shows that the metal ion not only is important for catalysis but also plays a structural role, holding together two lobes of the protein (*14*−*18*). Mutagenesis studies have shown that mutation of any of the three ligand residues causes either total loss of the metal and protein denaturation or severe reduction in affinity for the metal ion (*10*). Since E133A PDF is a well-behaved protein with a tightly bound metal ion over the pH range of 5.3−11.6, any change in the three protein ligands is highly unlikely. Indeed, the LMCT band was present under all pH conditions (pH 5.3−11.6). A major change in the metal complex geometry is also unlikely, as the same structural change would be expected to also take place in the wild-type PDF. We therefore conclude that the spectrum at acidic pH (<6.5) represents Co-PDF with a metal-bound water in the active site; as pH increases, the metal-bound water is ionized to form a metal-bound hydroxide under basic conditions (Scheme 2). Consistent with this assignment, the absorption spectrum of E133A PDF at basic pH is highly analogous to that of carbonic anhydrase at a similar pH, in which the involvement of Me^{2+}-OH in catalysis has been well-documented (*28*).

Anions such as Cl^- dramatically affect the spectral properties of E133A Co-PDF through direct binding to the metal ion. Although the Cl^- ion binds to the active-site metal 110 000-fold less tightly than a hydroxide ion, its affinity for the metal ion is 17 000-fold higher than that of a water molecule. Consequently, the presence of even a small amount of NaCl (e.g., 50 mM) in a protein sample results in essentially quantitative replacement of the metal-bound water by a chloride ion, and the observed spectral changes as a function of pH are actually due to the interconversion between metal-hydroxide and metal-chloride forms of PDF (Figure 2). Because of its higher affinity for the metal ion (as compared to water), Cl^- ions would be expected to increase the apparent pK_a for the metal-bound water molecule. This is precisely what we have observed: the addition of 50 mM NaCl shifted the pK_a value from 6.5 to 8.0 in E133A Co-PDF (compare Figure 2B and Figure 2D).

E133D Co-PDF has very similar spectral properties as the E133A mutant. Examination of its spectral changes with pH detected a single ionizing group with a pK_a < 6.5. Chloride ions perturb the E133D PDF spectrum in a similar manner as observed for the E133A mutant, but higher concentrations are required for the former. Analysis of its catalytic activity as a function of pH (in the presence of 2 M NaCl), however, revealed two ionization events in the enzyme active site, with

Scheme 2

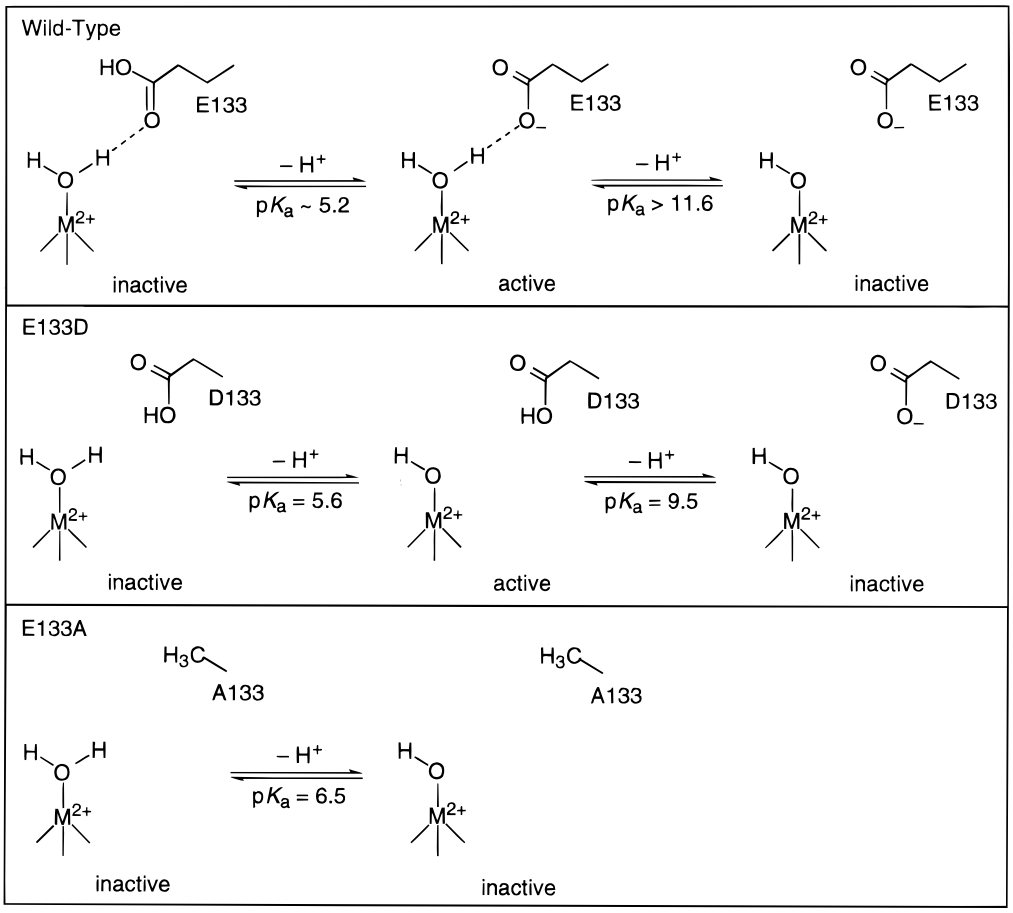

pK_a values of 7.3 and 9.5, respectively (Figure 1). We assign the first pK_a to the metal-bound water (Scheme 2); after subtracting the contribution by 2 M NaCl, the intrinsic pK_a for the water molecule was found to be 5.6, similar to that of E133A PDF (pK_a = 6.5). Deprotonation of the second ionizable group (pK_a = 9.5) inactivates the enzyme but does not cause any noticeable spectral perturbation. Since the second ionization event is missing in wild-type and presumably also E133A PDF (in the pH 5−11.6 range), we assign the second pK_a to Asp-133 in the mutant enzyme. Although a pK_a of 9.5 may seem too high for a carboxyl group, it is not without precedent. Rebek et al. (*30*) have synthesized a rigid model compound in which two carboxyl groups are forced to face each other at a ~3 Å distance. While the first pK_a of the diacid compound is 4.8, the second pK_a of the compound was found to be 11.1. In E133D PDF, the carboxyl group of Asp-133 is separated from the metal-bound hydroxide by ~4 Å [based on the 3 Å distance between Glu-133 and the metal-bound water in wild-type PDF (*15*−*17*)]. Therefore, electrostatic repulsion is likely responsible for the raised pK_a of Asp-133. Another factor that may also raise the pK_a is the fact that Asp-133 is situated in a hydrophobic environment. Since Asp-133 is probably not in direct bonding interaction (e.g., hydrogen bond) with the metal complex, its ionization should not affect the ligand identity or geometry of the metal center and therefore does not change the absorption spectrum.

For wild-type PDF, pH profiles derived from both spectral and catalytic properties are identical and exhibit a single ionization event with a pK_a of ~5.2 (Figures 1 and 2). The flat pH profile over the pH range of 6−11.6 suggests that the second pK_a is >11.6. We have also found that wild-type PDF is much less susceptible to chloride inhibition than either of the E133 mutants. In the X-ray crystal structure, the metal-bound water/hydroxide is hydrogen bonded to Glu-133, sharing a proton between the two oxygen atoms (*15*−*17*). Because the absorption spectrum of wild-type PDF at neutral pH closely resembles the E133A PDF spectrum at pH 5.3 (Figure 2D), the shared proton should lie closer to the metal-bound oxygen than Glu-133, and, therefore, the wild-type PDF is effectively in the metal-bound water form (Scheme 2). Removal of the shared proton would lose the favorable hydrogen-bonding interaction and generate two anionic species (the metal-bound hydroxide and the carboxylate of Glu-133) at a short distance (~3 Å), causing strong electrostatic repulsion, hence the exceptionally high second pK_a (>11.6). Under acidic conditions (pH <5), a proton is added to the metal−water−carboxylate unit, resulting in the protonation of Glu-133 and inactivation of the enzyme. This model explains many of the observed properties. For example, when the distance between the metal-bound water and the carboxyl group is increased in E133D PDF, the second pK_a decreases to 9.5. Cl^- ions readily replace the metal-bound water/hydroxide in the E133D and E133A mutants and inhibit the mutant enzymes, whereas they have little effect on the wild-type enzyme (at neutral pH). This is because the metal-bound water is hydrogen bonded to Glu-133 and therefore more tightly bound in the wild-type enzyme. Similarly, thiorphan has 7-fold higher affinity to the E133 mutants than wild-type PDF because thiorphan

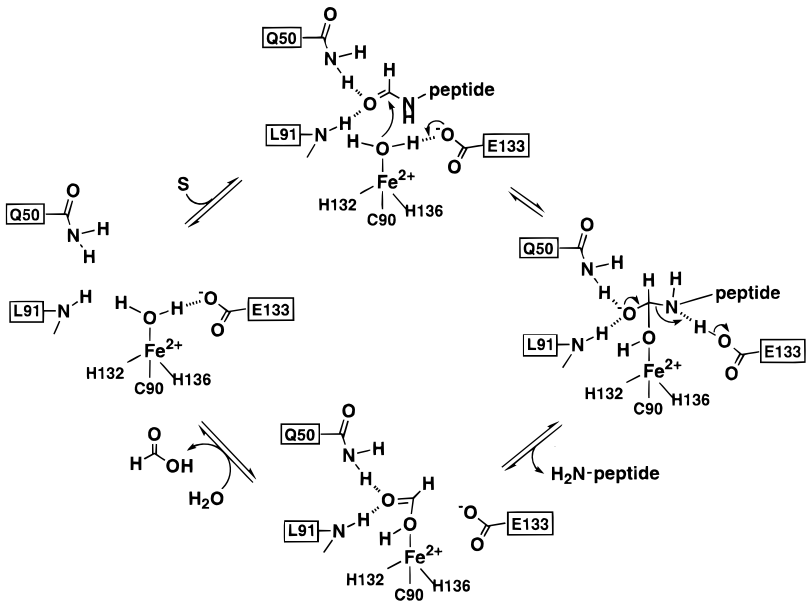

FIGURE 6: Proposed catalytic mechanism for PDF.

binding requires the displacement of the metal-bound water/hydroxide by the thiorphan thiol group. In a striking parallel, Co(II)-substituted carboxypeptidase A, in which the metal-bound water is hydrogen bonded to the catalytic residue Glu-270, is also insensitive to pH (*31*). Upon modification of Glu-270 with carbodiimide, however, the carboxypeptidase became highly sensitive to pH or the addition of anions such as the Cl^- ion.

Function of the Metal. The importance of a divalent metal ion for PDF function is underscored by the total lack of activity or folding in its absence (*12, 13*). Substitution of Zn^{2+} for Fe^{2+} leads to a highly stable protein that is again structurally indistinguishable from the native enzyme by X-ray crystallography and yet results in a decrease in catalytic activity by more than 2 orders of magnitude, suggesting the direct involvement of the metal ion in catalysis (*11, 17*). Two possible functions have been proposed for zinc metallopeptidases (*32*). The metal ion may act to lower the pK_a of its bound water, as has been observed in PDF. Alternatively, the metal ion may act as a Lewis acid, polarizing the carbonyl bond so that it becomes more susceptible to nucleophilic attack by a water molecule. While for several extensively studied zinc enzymes (e.g., carboxypeptidase A and thermolysin) the function of the metal is generally believed to be deprotonation of the water nucleophile or a combination of both functions, a reverse protonation mechanism has been proposed, in which the sole function of the metal is to activate the carbonyl of a scissile amide bond (*33, 34*). In the reverse protonation mechanism, the metal-bound water form is the catalytically active form, and upon substrate binding, the metal-coordinated water is replaced by the substrate carbonyl group. Such a mechanism predicts that the K_M value would be highly pH dependent and increase with pH, which is indeed true for both carboxypeptidase A and thermolysin (*33, 34*).

In PDF, the metal ion functions primarily to deprotonate the water molecule. First, the pK_a of the metal-bound water in E133A PDF is 6.5. In the absence of Glu-133, no other protein side chain in the PDF active site is capable of strongly influencing the acidity of the metal-bound water. We therefore conclude that the metal ion is primarily responsible for the 8 orders of magnitude reduction in the pK_a of water in E133A PDF. Second, the electronic absorption spectrum of Co^{2+} ions is very sensitive to changes in its ligand identity or geometry. As described above, conversion of the metal-hydroxide form to either metal-Cl^- form or a metal-H_2O form resulted in dramatic spectral changes. Distinctive spectral changes have also been observed when either the wild-type or the E133A, E133D mutants were mixed with thiorphan, ML-*p*NA (a competitive inhibitor with $K_I = 18\ \mu$M to wild-type Co-PDF), or *N*-(2-hydroxycaproyl)lysyl-*p*-nitroanilide (a competitive inhibitor with $K_I = 4.6\ \mu$M to wild-type Co-PDF) (results not shown). However, the addition of saturating concentrations of a substrate (f-ML-*p*NA) to E133A PDF induced little spectral changes at either acidic or basic pH (Figure 5). This result suggests that substrate binding does not change the ligand environment and therefore the formyl carbonyl is not coordinated to the metal ion in the E·S complex. Third, the X-ray crystal structure of PDF bound with a tetrahedral H-phosphonate transition-state analogue shows that only one of the two nonbridging phosphonate oxygen atoms is coordinated with the metal ion, replacing the metal-bound water in the native structure (*18*). The second phosphonate oxygen of the inhibitor is pointed away from the metal and Glu-133 and is instead hydrogen bonded to the main-chain NH of Leu-91 and the side-chain NH_2 of Gln-50. This is consistent with the metal-hydroxide mechanism, with the metal-bound oxygen derived from the hydroxide nucleophile and the second oxygen derived from the carbonyl group. The Lewis acid mechanism would require nucleophilic attack by an unactivated water molecule. Finally, the K_M values of both wild-type and E133D PDF are pH independent. This result is consistent with the notion that substrate binding does not involve carbonyl coordination to the metal ion. It rules out a reverse protonation mechanism for PDF.

Function of Glu-133. In principle, Glu-133 may help ionize the metal-bound water by abstracting one of the water protons (as a general base) and/or facilitate product formation by protonating the leaving −NHR group (as a general acid).

Since the metal-bound water in E133A PDF has a pK_a of 6.5 and Asp-133 in the catalytically active form of E133D PDF is in the protonated state (Figure 1 and Scheme 2), a general base function for Glu-133 (Asp-133) is unlikely or at least not critical during catalysis. However, since the E133A mutant is catalytically inactive, Glu-133 (Asp-133) must be required as a general acid donating a proton to the leaving amide ion. Presumably, the nucleophilic addition of the metal-bound hydroxide to the formyl carbonyl can still take place in the E133A mutant, but the tetrahedral intermediate can only collapse back to the substrate because formation of the negatively charged −NHR product is energetically disfavored in the absence of the general acid. Glu-133 may also stabilize the transition states through hydrogen bonding interactions.

Catalytic Mechanism. Figure 6 illustrates our proposed mechanism for PDF. In the free enzyme, the metal-bound water is hydrogen bonded to Glu-133. In the E·S complex, the formyl carbonyl group is placed next to the metal-bound water. Because the pK_a values for the metal-bound water (6.5) and the carboxyl group of Glu-133 (∼5) are similar, the shared proton may be readily transferred from the water molecule to the carboxylate generating the metal-bound hydroxide, which attacks the formyl carbonyl group. In the tetrahedral intermediate, the oxyanion derived from the carbonyl group forms hydrogen bonds with the backbone NH of Leu-91 and the side-chain NH_2 of Gln-50, whereas the other oxygen is ligated to the metal ion. Decomposition of the tetrahedral intermediate proceeds by the re-formation of the original C═O bond, and during the second transition state, the leaving NHR group is likely hydrogen bonded to Glu-133. Transfer of the proton from Glu-133 to the −HNR group and subsequent water−formate exchange complete the catalytic cycle.

We have previously noted significant similarities in the active-site structure between peptide deformylase and thermolysin (*15*). While we have not seen any evidence for a Lewis acid role of the metal ion in PDF, substantial evidence for Lewis acid catalysis has been accumulated in the case of thermolysin (*32*). One might speculate that the two enzymes have evolved to use slightly different mechanisms because of their different physiological functions. The carbonyl in a formyl group is intrinsically more susceptible to nucleophilic attack than the carbonyl in a peptide bond, due to lack of an electron-donating α-carbon atom. Indeed, peptide deformylase has little activity toward *N*-acetylated peptides (*2, 8*). Although steric hindrance plays a role, the electronic effect is clearly an important factor since difluoroacetylated peptides are efficiently hydrolyzed by peptide deformylase (*35*). While a nucleophilic metal-hydroxide is all it takes to cleave a formamide bond, a more elaborate system is probably necessary to hydrolyze the inherently less reactive peptide bond.

REFERENCES

1. Meinnel, T., Mechulam, Y., and Blanquet, S. (1993) *Biochimie 75*, 1061−1075.
2. Adams, J. M. (1968) *J. Mol. Biol. 33*, 571−589.
3. Livingston, D. M., and Leder, P. (1968) *Biochemistry 8*, 435−443.
4. Takeda, M., and Webster, R. E. (1968) *Proc. Natl. Acad. Sci. U.S.A. 60*, 1487−1494.
5. Mazel, D., Pochet, S., and Marliere, P. (1994) *EMBO J. 13*, 914−923.
6. Meinnel, T., and Blanquet, S. (1994) *J. Bacteriol. 176*, 7387−7390.
7. Dardel, F., Ragusa, S., Lazennec, C., Blanquet, S., and Meinnel, T. (1998) *J. Mol. Biol. 280*, 501−513.
8. Rajagopalan, P. T. R., Datta, A., and Pei, D. (1997) *Biochemistry 36*, 13910−13918.
9. Groche, D., Becker, A., Schlichting, I., Kabasch, W., Schultz, S., and Wagner, A. F. V. (1998) *Biochem. Biophys. Res. Commun. 246*, 342−346.
10. Meinnel, T., Lazennec, C., and Blanquet, S. (1995) *J. Mol. Biol. 254*, 175−183.
11. Rajagopalan, P. T. R., Yu, X. C., and Pei, D. (1997) *J. Am. Chem. Soc. 119*, 12418−12419.
12. Rajagopalan, P. T. R., and Pei, D. (1998) *J. Biol. Chem. 273*, 22305−22310.
13. Ragusa, S., Blanquet, S., and Meinnel, T. (1998) *J. Mol. Biol. 280*, 515−523.
14. Meinnel, T., Blanquet, S., and Dardel, F. (1996) *J. Mol. Biol. 262*, 375−386.
15. Chan, M. K., Gong, W., Rajagopalan, P. T. R., Hao, B., Tsai, C. M., and Pei, D. (1997) *Biochemistry 36*, 13904−13909.
16. Becker, A., Schlichting, I., Kabsch, W., Schultz, S., and Wagner, A. F. V. (1998) *J. Biol. Chem. 273*, 11413−11416.
17. Becker, A., Schlichting, I., Kabsch, W., Groche, D., Schultz, S., and Wagner, A. F. (1998) *Nat. Struct. Biol. 5*, 1053−1058.
18. Hao, B., Gong, W., Rajagopalan, P. T. R., Zhou, Y., Pei, D., and Chan, M. K. (1999) *Biochemistry 38*, 4712−4719.
19. Kunkel, T. A., Roberts, J. D., and Zakour, R. A. (1987) *Methods Enzymol. 154*, 367−382.
20. Wei, Y., and Pei, D. (1997) *Anal. Biochem. 250*, 29−35.
21. Guo, X.-C., Rajagopalan, P. T. R., and Pei, D. (1999) *Anal. Biochem. 273*, 298−304.
22. Meinnel, T., Lazennec, C., Dardel, F., Schmitter, J.-M., and Blanquet, S. (1996) *FEBS Lett. 385*, 91−95.
23. Hochuli, E., Dobeli, H., and Schacher, A. (1987) *J. Chromatogr. 411*, 177−184.
24. Hu, Y.-J., Rajagopalan, P. T. R., and Pei, D. (1998) *Bioorg. Med. Chem. Lett. 8*, 2479−2482.
25. Schimmel, P. (1989) *Acc. Chem. Rev. 22*, 232−233.
26. Maret, W., and Vallee, B. (1993) *Methods Enzymol. 226*, 52−71.
27. Bertini, I. (1983) in *Coordination Chemistry of Metalloenzymes*, *I* (Bertini et al., Eds.) pp 1−18, D. Reidel Publishing Company, Dordrecht, The Netherlands.
28. Lindskog, S. (1983) in *Zinc Enzymes* (Spiro, T. G., Ed.) pp 79−121, Wiley & Sons, New York.
29. Meinnel, T., Patiny, L., Ragusa, S., and Blanquet, S. (1999) *Biochemistry 38*, 4287−4295.
30. Rebek, J., Jr., Duff, R. J., Gordon, W. E., and Parris, K. (1986) *J. Am. Chem. Soc. 108*, 6068−6069.
31. Vallee, B., Glades, A., Auld, D. S., and Riordan, J. F. (1983) in *Zinc Enzymes* (Spiro, T. G., Ed.) pp 27−75,Wiley & Sons, New York.
32. Lipscomb, W. N., and Sträter, N. (1996) *Chem. Rev. 96*, 2375−2433.
33. Mock, W. L., and Zhang, J. Z. (1991) *J. Biol. Chem. 266*, 6393−6400.
34. Mock, W. L., and Stanford, D. J. (1996) *Biochemistry 35*, 7369−7377.
35. Hu, Y.-J., Wei, Y., Zhou, Y., Rajagopalan, P. T. R., and Pei, D. (1999) *Biochemistry 38*, 643−650.

BI9919899